

PAPER • OPEN ACCESS

Development of a low-cost EMG-data acquisition armband to control an above-elbow prosthesis

To cite this article: Christoph Schlüter *et al* 2022 *J. Phys.: Conf. Ser.* **2232** 012019

View the [article online](#) for updates and enhancements.

You may also like

- [Estimating muscle activation from EMG using deep learning-based dynamical systems models](#)
Lahiru N Wimalasena, Jonas F Braun, Mohammad Reza Keshtkaran *et al.*
- [Online adaptive neural control of a robotic lower limb prosthesis](#)
J A Spanias, A M Simon, S B Finucane *et al.*
- [The effect of involuntary motor activity on myoelectric pattern recognition: a case study with chronic stroke patients](#)
Xu Zhang, Yun Li, Xiang Chen *et al.*



ECS Membership = Connection

ECS membership connects you to the electrochemical community:

- Facilitate your research and discovery through ECS meetings which convene scientists from around the world;
- Access professional support through your lifetime career;
- Open up mentorship opportunities across the stages of your career;
- Build relationships that nurture partnership, teamwork—and success!

Join ECS!

Visit electrochem.org/join



Development of a low-cost EMG-data acquisition armband to control an above-elbow prosthesis

Christoph Schlüter¹, Washington Caraguay² and Doris Cáliz Ramos^{3,*}

¹Faculty of Mechanical Engineering, Karlsruher Institut für Technologie, Germany

²Faculty of Electronic, Computer and Telecommunication Engineering, Espíritu Santo University, Ecuador

³Pervasive Computing Systems / TECO, Karlsruher Institut für Technologie, Germany

caliz@teco.edu

Abstract. This work presents the development and implementation of an armband for EMG-data acquisition of the upper arm. The developed prototype serves for investigations on EMG-signal processing with the final objective of reliably controlling a prosthesis for a transhumeral amputee. To make the product available for a greatest possible number of people one of the main characteristics will be a design of very low cost. A focus is put on the electric circuit design. In order to manufacture the prototype without difficulties, it is exclusively designed with components, which are available on the Ecuadorian market. The development is based on previous investigations and approaches of other researchers. With help of electric circuit simulations, the design was adapted and optimized step by step and a reliable low-noise circuit was established. All components are arranged on printed circuit boards in a way to keep the device as small as possible. To optimally avoid noise the length of the connection from the electrodes to the amplifier is minimized. Compact 3D-printed housings cover all the electric components. All housings consist of only two parts and are intuitive to assemble. Holes in the bottom offer space to fix electrodes via a snap-fastener connection. 3D-printed elastic straps are designed to connect the subsystems and hold the device in place. The armband including two sensors weighs 92 g and is capable of measuring two muscles with a bipolar EMG-setting each, sharing one reference electrode, which is aligned on the side of the upper arm between the biceps and triceps muscles. The amplification of the sensors is adjustable individually by potentiometers, facilitating a gain factor range of 211 to 2016 V/V. The data is recorded by a microcontroller board and send to a computer for processing via wire or Bluetooth. For wireless operation, rechargeable batteries are integrated. Test measurements on an able-bodied human prove the functionality of the device.



1. Introduction

1.1. Motivation and goal setting

The goal of this project is to develop an economic alternative to existing high-tech solutions with the aim of making the technology available for people with low financial backing, especially people living in Ecuador and other third world countries. It shall be designed using components available in the local market to conveniently serve the domestic demand. The prosthetic arm shall facilitate disabled people's lives and help them to deal with daily challenges more comfortably and autonomously. It shall be controlled by the residual muscles' contraction, which is achieved by measuring the EMG-activity of those muscles. This work in particular will focus on the development of a device for EMG-signal acquisition of residual muscles for transhumeral amputees, establishing an easy setup and wearable device.

The actual market offers various products, both prosthetic arms and EMG-signal amplification and interpretation devices, but none of them meet the expectations exactly. Lots of commercial products are high prized or include non-reusable components [1]. On top of that it is to be mentioned that Ecuador's market is very restricted, so one big problem is that a lot of parts are hardly available and need time consuming and expensive shipping. Here a way is presented to build a simple EMG-data acquisition armband with parts freely available on the Ecuadorian market.

1.2. Requirements for the EMG-acquisition armband

According to the set specifications and the previous research several important characteristics and requirements for the device were derived. As key features it has been defined, that all components shall be available in Ecuador and the product has a cost well below similar currently purchasable products. Another important characteristic is the signal quality. Low noise is expected and all occurring frequencies must be recorded. These are all frequencies between 5 and 500 Hz [2]. The armband must be easy to put on, intuitive to place to the right location and hold firmly on the arm. It is important to be worn comfortably for several hours and shall be entirely reusable. Therefore it should neither be too heavy, nor too big. An upper limit for the weight was set to 200 g. As people's bodies vary from person to person and every amputee has different residual muscles an adaptable solution is looked for.

1.3. Production of the EMG-signal

EMG is to measure skeletal muscle activity. Skeletal muscles consist of parallel arranged muscle fiber bundles which can be divided into single muscle fibers to which motor endplates are attached [3]. Motor endplates are synapses that receive electrical signals from the nervous system. In resting muscle cells there is a potential difference of about -80 mV between the inside and the outside, caused by an ion imbalance, called resting potential. EMG-signals are action potentials in the muscle fiber occurring when contracting a muscle. These potentials can even be determined at the surface of the skin. In the upper arm there are two individually contractible muscle groups, the biceps and the triceps. For people with transhumeral amputation or elbow exarticulation these muscles often remain partially. As they cannot serve the function of flexing the forearm anymore, they can be used to control a prosthetic arm [4].

1.4. EMG-signal acquisition

As the developed device shall be suitable for everyday use, this work will not take intrusive methods of capturing EMG-signals into account and focus on surface EMG (SEMG), for which usually two surface electrodes are placed on the skin over the muscle which is to investigate. The SEMG sensor measures the potential difference between those two electrodes which is the result of a superposition of all the underlying action potentials. This technique can only give satisfactory results for superficially aligned muscles. [2]

The signal quality of the measurement is very important for the evaluation and is influenced by many factors. One is the tissue properties which determine how good the potential is conducted to the skin. This factor can vary a lot from person to person. Another factor is the contact between skin and electrode, which depends a lot on the skin properties, but also on the electrode properties. For ideal conducting conditions the skin should be depilated and cleaned with an appropriate cleansing agent or alcohol. Especially in medical uses conductive gel is usually applied between electrode and skin to reduce the impedance. As the EMG-signal is of low voltage several unwanted interferences easily enter the measurement and add noise to the signal. Most interference originates from powerlines and results in noise at the powerline's frequency and its harmonics [2], which in Ecuador are multiples of 60 Hz. In order to avoid these interferences, the cable to the amplifier should be kept short. A proper housing and isolation also help to suppress such interferences. [5]

In a bipolar setting the electrode's voltage difference is amplified. As the action potential peaks pass both electrodes one by one, first a positive and then a negative peak will be detected, so the whole signal is zero-mean and a probably occurring offset and common-mode noise can be removed easily. [6]

2. System design

The captured signal needs to be amplified and conditioned for digitalization with an Analog-Digital Converter (ADC). The digitalized signal is preprocessed by a microcontroller, which acts as the core of the device. It preprocesses the data to pass it over to a computer via Bluetooth. The whole device is powered by a battery to be operated wirelessly and needs to be rechargeable. A structure of the electric circuit is given in Figure 1 and the four mechanical subsystems into which the device is divided are indicated by different colors. As depicted the armband includes five electrodes to make the measurements. In this project the spots specified by the SENIAM project [7], to locate the electrodes for tests on able-bodied humans were used.

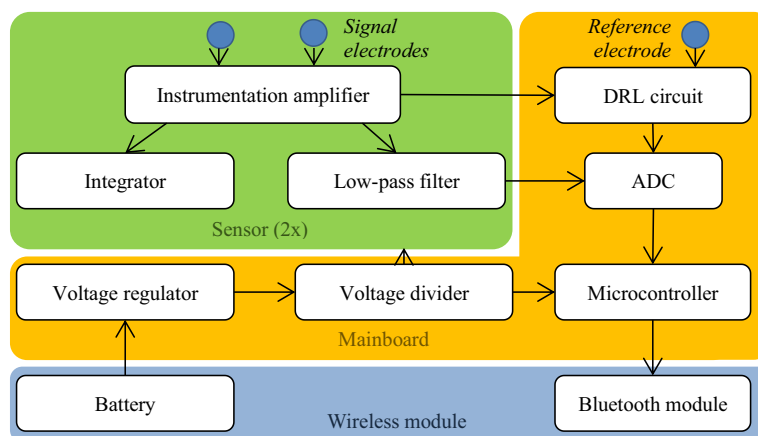


Figure 1. Electrical structure and partition into mechanical subsystems.

2.1. Electric circuit design

The electric circuit was designed observing several existing solutions [8-10], simulating circuit designs and testing new circuits on a breadboard on an able-body human. The system can be separated into sub-circuits which will be explained one by one in this chapter. All resistors used, excluding the gain resistors, are chosen with high resistance values above 10 k Ω to keep the currents and therewith the power consumption of the device low.

2.1.1. Instrumentation amplifier. One of the main components of the electric circuit, which was focused on, is the Instrumentation Amplifier (InAmp), which needs to meet several specifications to give the wanted results. An integrated Instrumentation Amplifier is used as this is the most promising and space efficient approach. Out of many the AD620 from Analog Devices was chosen as it was the only one available on the Ecuadorian market and meets the requirements excellently. It has a CMRR, higher than the recommended minimum value of 95 dB [2] and supports a gain range of 1-10000 V/V, which is more than sufficient for this application and adjustable through a gain resistor. It has a comparably low power consumption, which is important with respect to battery life and has a high input impedance of 100 G Ω .

2.1.2. Potential levels. The whole circuit needs three constant fundamental potential levels, the ground level, and a positive and a negative potential to power the OpAmps and the Instrumentation Amplifiers. In the following they will be called GND, Vcc and Vee respectively. The third potential for the amplification circuit is created with a voltage divider, illustrated in Figure 2. To keep the current through the resistors low and so do not waste battery power, high resistances of 1 M Ω are chosen. A voltage follower is added to make the resulting voltage independent to the load. The advantage of this circuit is that no extra circuit is needed to lift the voltage into a measuring range like in [10] as the Arduino always measures input voltages referring it to its own ground, which in this setup is Vee. All voltages occurring are between 0 and 5 V and oscillate around 2.5 V referring them to Arduino's ground.

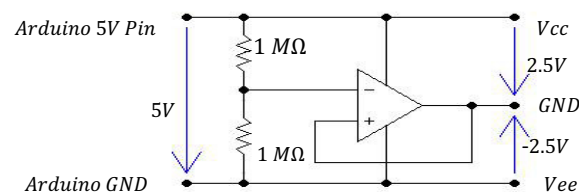


Figure 2. Voltage divider for defining the GND potential.

2.1.3. Integrator circuit. This circuit is presented in the datasheet of the Instrumentation Amplifier INA114 by Texas Instruments [11], and represents a control loop to eliminate offset voltages. It feeds the inverted integrated Output voltage back to the reference pin of the instrumentation amplifier, making advantage of the fact that the EMG-signal is zero-mean and so, its integral is also zero. As this circuit acts as a high-pass filter and can attenuate low-frequency fluctuations the response time has to be adjusted. The proposed input resistance in [11], R_{int} of 1 M Ω and a capacitor C_{int} of 100 nF provide a cut-off frequency of 1.59 Hz and have not been adjusted due to appropriate results.

2.1.4. Driven right leg circuit. In bipolar EMG measurements a DRL circuit is needed to match the potential on the skin to the inverting amplifier's reference of the InAmp. The DRL circuit is attached to a reference electrode, which is conventionally placed on an electrically inactive part of the body. A standard circuit design was presented by Bruce B. Winter and John G. Webster back in 1983 [12]. But in this case the reference electrode shall as well be integrated into the armband to not have a cable coming out of it and struggling with fixture of the electrode on the arm. That means that the reference electrode will not align on an electrically inactive part of the body but on muscle tissue. The design presented by Winter and Webster was used in combination with a frequency compensated OpAmp which leads to very promising results. Winter and Webster derive the formula for the effective resistance of the DRL-circuit to the body. According to that the relation of R_{DRL} to R_G has to be chosen high in order to set the effective resistance low. [12] As R_G is defined by the gain factor, only R_{DRL} can be adjusted and is set to 1 M Ω .

2.1.5. Low pass filter. As the frequencies in an EMG-signal do not exceed 500 Hz, all occurring frequencies above can be considered unwanted noise. These are suppressed with an amplifying inverting low-pass filter at the output of the circuit with a cut-off frequency ω_0 of about 500 Hz. A 33 k Ω resistance and 10 nF capacitor are economic standard components and lead to very satisfying results.

$$\omega_0 = \frac{1}{2\pi R_{TP,2} C_{TP}} = 482.29 \text{ Hz} \quad (1)$$

This circuit additionally fulfils the function of a second gain stage, which's gain factor is adjusted by the input impedance. This is important because the AD620 has a comparably low voltage output swing and is only able to display an output range of 2.7 V. This represents only little more than half of the available measuring range, so it makes sense to perform only a half of the amplification with the AD620 and use the second gain stage with a greater output swing to amplify by the factor 2. Rail-to-Rail (R2R) OpAmps are especially optimized on a great output swing and should be used in this application. Unfortunately, there could not be found any dual Rail-to-Rail OpAmp in Ecuador, so the LM358 is used, accepting a loss in the voltage output range. The gain of this second amplification stage was realized with an input resistance of 18 k Ω , which is the closest standard resistance to the half of 33 k Ω , to achieve a gain factor of 1.83 V/V.

A Bode plot of the whole circuit is given in Figure 3. It clearly shows the expected bandpass with cut-off frequencies of 1.60 Hz and 451.76 Hz.

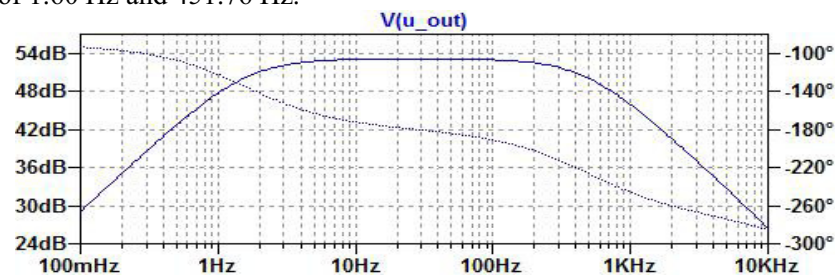


Figure 3. Bode plot of the simulated circuit.

2.1.6. Gain resistance. People's skin conditions and tissue properties vary a lot from person to person [2], so it is important to design a solution which allows the adjustment of the amplification factor. Therefore there are four gain resistors scheduled. R_{g1} and R_{g2} have the same resistance and are connected in series to create the reference potential for the DRL circuit at their common node. R_{g3} and R_{g4} are connected serially, parallel to R_{g1} and R_{g2} . R_{g4} is a potentiometer, which is used to adjust the gain factor. It is adjustable from 0 to 500 Ω . The arrangement of the gain resistors is sketched in Figure 4.

$$\text{gain resistance: } R_G(R_{g4}) = \frac{2 \cdot R_{g1} (R_{g3} + R_{g4})}{2R_{g1} + R_{g3} + R_{g4}} \quad (2)$$

$$\text{gain: } G(R_{g4}) = \frac{49400\Omega \cdot 2 \cdot R_{g1} + R_{g3} + R_{g4}}{2 \cdot R_{g1} (R_{g3} + R_{g4})} + 1 \quad (3)$$

R_{g1} and R_{g2} are set to 1 k Ω , R_{g3} to 47 Ω in order to restrict the gain resistance to values between $R_G(R_{g4} = 0\Omega) = 46.0\Omega$ and $R_G(R_{g4} = 500\Omega) = 429.5\Omega$ and the gain factor for the first gain stage to values between $G(R_{g4} = 500) = 115$ and $G(R_{g4} = 500) = 1100$. For the entire circuit this results in a gain factor range from 210.83 to 2016.67 V/V.

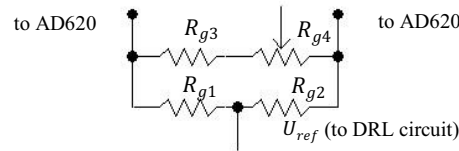


Figure 4. Arrangement of the gain resistors.

2.1.7. Mechanical design. To hold all components together and fix the armband on the arm, defining the electrodes' positions, the device was divided into four physically separated, individually housed subsystems connected by cables and elastic straps. Two identical sensors are aligned on different sides of the arm. The circuit boards of the two sensors include the amplification circuit, integrator circuit and low-pass filter each. The inter-electrode distance is 21.5 mm in order to place the instrumentation amplifier in between. The developed sensor is shown in Figure 5. Each sensor offers two snap-fastener sockets. As many electrodes are sold with a snap-fastener connection it was decided to arm snap-fastener sockets directly to the circuit boards. This design has the advantage that the electrodes are exchangeable, so any purchasable electrodes with a snap-fastener connection, even pre-gelled ones, can be inserted. Two different Ag/AgCl electrodes from 3M Health Care and HeartRode have been tested successfully. To distribute the weight around the arm and keep the armband as flat as possible there is a third circuit board between the sensors where the microcontroller will be fixed on. All circuits that only appear once, namely the microcontroller board, the DRL circuit and the voltage divider are united on this third board, in the following called main board. In the center of the board a snap-fastener socket for the reference electrode is placed. The whole board has a size of 45x29 mm² and is shown in Figure 5. The batteries and the Bluetooth module make a fourth subsystem fixed opposite the main board. It is only needed when the device is operated wirelessly.

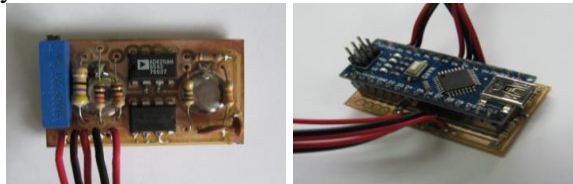


Figure 5. Sensor circuit board (left) and Main board (right).

As housings 3D-printable designs are chosen for the prototypes. They are all divided in two parts with rails to slide into each other and offer openings for the cables, connectors and electrodes. Little hooks on the sides allow to attach elastic straps to hold the measuring devices in place as shown in Figure 6.



Figure 6. Housings for mainboard (left), sensors (center) and batteries and Bluetooth module (right)

To make the armband useable for people with different arm circumferences the parts are exchangeable. Different elastic strap lengths can freely be combined to place the sensors on the right spots and ensure an appropriate contact pressure and wearing comfort.

3. Evaluation of the system

The sensors weigh 16 g each, the case with the main board 26.5 g and the battery box 28 g. Together with the armband and cables it reaches a total weight of 92 g. All subsystems and therewith the armband are shorter than 50 mm. This is considered reasonable. Whereas the sensors are very flat, the box for the main board is high with 22 mm. This is due to the socket the Arduino Nano is placed on and can be reduced soldering the microcontroller board directly to the PCB.

The total material costs for the device are below \$55, but it can be observed that the batteries, the InAmp, the Arduino and the Bluetooth module make more than 75% of the costs, whereas other electrical components and the material prices do not have such a great impact and the price for many components can be reduced by quantity discounts. Several test measurements have been performed on a voluntary, able-bodied test person as seen in Figure 7. For a loose armband or working in a very dry environment it can be necessary to apply conductive gel to the electrodes to get conclusive measurements.



Figure 7. Tests on an able-bodied test person.

In the performed tests the skin was not epilated, and conductive gel was not applied either. The gain resistances of the sensors on the biceps and triceps were tuned to 241 Ω and to 128 Ω respectively, leading to gain factors of 377,63 V/V and 709.39 V/V. These values were adjusted during a measurement with the strongest muscle contraction possible to perfectly use the available measuring range. The triceps displayed a lower EMG-signal than the biceps and is therefore amplified more. The tests showed a very low noise level of 22.3 mV for the sensor on the biceps and 32.7 mV for the one on the triceps. A test measurement is given in Figure 8 contracting both muscles at the same time for about 1.2 seconds.

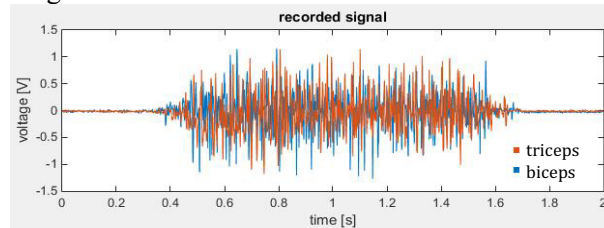


Figure 8. EMG-measurement on able-bodied human.

4. Conclusions

In summary it can be concluded that the prototype satisfies the requirements in many points but still has the necessity to be optimized in several aspects. An adaptable, comfortable solution, which holds firmly on the upper arm was found. It is assemblable with components available in Ecuador and the noise level is satisfactory low. The dimensions are comparably big and should be reduced for following prototypes. The prototype is lower priced than actual purchasable products. Its price is raised by very few expensive components, which should be tried to replace or cheaper sellers should be found.

This work shows the importance of suppressing noise before the first amplification stage to avoid unnecessary filtering and record the pure EMG-signal. This is realized by the very short and stiff connection of the electrodes to the amplifier. Many papers focus on the combination and selection of

complex, suitable filters, whereas this prototype provides a low-noise EMG-signal with very simple first-order filters.

5. Outlook

The developed device uses very low currents, therefore for further improvements surface-mount electrical components should be considered to scale it down to a fraction of the actual size. This adjustment will not only make the device smaller but also lighter and most probably cheaper. Furthermore, the armband will slip even less as with the weight also the inertial forces will be reduced. Next the device must be tested on people with a transhumeral amputation to prove the functionality and verify the product.

As a further step the captured signal needs to be processed and relevant features must be extracted. There are many different approaches. Usually, the signal is rectified as there is no interest in the polarity of the peaks and different averaging procedures can be applied to the rectified signal. The averaged, rectified signal can be used to distinguish between different contraction levels or for a linear control of an articulation. A promising approach is a pattern recognition based on an artificial intelligence. For this a big number of samples and intended movements of various test persons will be needed. The Arduino is very limited in terms of computing power and intensive processing algorithms have to be performed on an additional device. Computer software should be developed to simulate arm movements and verify how many movements can be safely distinguished with the recorded data. The software can also serve to train an amputee, to learn how to use the residual muscles to perform a maximum number of tasks.

References

- [1] W. Caraguay, M. Sotomayor, C. Schlüter, and D. Caliz, *Assistive Technology in Ecuador: Current Status of Myoelectric Prostheses of Upper Limbs*, vol. 1066. 2020.
- [2] P. Konrad, "EMG-FIBEL Eine praxisorientierte Einführung in die kinesiologicalische Elektromyographie," *Noraxon INC. USA*, vol. 1, 2005.
- [3] C. Clauss and W. Clauss, *Humanbiologie kompakt*, 2nd ed. Gießen: Springer-Verlag GmbH Deutschland, 2018.
- [4] K. Zuo and J. Olson, "The evolution of functional hand replacement: From iron prostheses to hand transplantation," *Can. J. Plast. Surg.*, vol. 22, no. 1, pp. 44–51, 2014.
- [5] B. Milosevic, S. Benatti, and E. Farella, "Design challenges for wearable EMG applications," *Proc. 2017 Des. Autom. Test Eur. DATE 2017*, pp. 1432–1437, 2017.
- [6] T. Beck *et al.*, "A comparison of monopolar and bipolar recording techniques for examining the patterns of responses for electromyographic amplitude and mean power frequency versus isometric torque for the vastus lateralis muscle," *J. Neurosci. Methods*, vol. 166, no. 2, pp. 159–167, 2007.
- [7] "SENIAM (surface EMG for non-invasive assessment of muscles)." .
- [8] M. H. Khan *et al.*, "Design of low cost and portable EMG circuitry for use in active prosthesis applications," *2012 Int. Conf. Robot. Artif. Intell. ICRAI 2012*, pp. 204–207, 2012.
- [9] U. Imtiaz *et al.*, "Design of a wireless miniature low cost EMG sensor using gold plated dry electrodes for biomechanics research," in *2013 IEEE International Conference on Mechatronics and Automation, IEEE ICMA 2013*, 2013, pp. 957–962.
- [10] A. Beneteau, G. Di Caterina, L. Petropoulakis, and J. Soraghan, "Low-cost wireless surface EMG sensor using the MSP430 microcontroller," *EDERC 2014 - Proc. 6th Eur. Embed. Des. Educ. Res. Conf.*, pp. 264–268, 2014.
- [11] T. Instruments, "INA114," *Precision Instrumentation Amplifier. Datasheet*, 2018. .
- [12] B. Winter and J. Webster, "Driven-Right-Leg Circuit Design," *IEEE Trans. Biomed. Eng.*, vol. BME-30, no. 1, pp. 62–66, 1983.